JOURNAL OF AGRICULTURAL AND FOOD CHEMISTRY

ARTICLE

pubs.acs.org/JAFC

Molecular Binding of Black Tea Theaflavins to Biological Membranes: Relationship to Bioactivities

Timothy W. Sirk,*[,†] Mendel Friedman,[‡] and Eugene F. Brown[§]

[†]Macromolecular Science & Technology Branch, U.S. Army Research Laboratory, Aberdeen, Maryland 21005-5069, United States

[‡]Western Regional Research Center, Agricultural Research Service, U.S. Department of Agriculture, Albany, California 94710, United States

[§]Department of Mechanical Engineering, Virginia Polytechnic Institute and State University, Blacksburg, Virginia 24061, United States

ABSTRACT: Molecular dynamics simulations were used to study the interactions of three theaflavin compounds with lipid bilayers. Experimental studies have linked theaflavins to beneficial health effects, some of which are related to interactions with the cell membrane. The molecular interaction of theaflavins with membranes was explored by simulating the interactions of three theaflavin molecules (theaflavin, theaflavin-3-gallate, and theaflavin-3,3′-digallate) with a mixed bilayer composed of 1-palmitoyl-2-oleoyl phosphatidylcholine (POPC) and 1-palmitoyl-2-oleoyl phosphatidylethanolamine (POPE). The simulations show that the theaflavins evaluated have an affinity for the lipid bilayer surface via hydrogen bonding. The molecular structure of theaflavins influenced their configuration when binding to the bilayer surface, as well as their ability to form hydrogen bonds with the lipid headgroups. The theaflavin−bilayer interactions studied here help to define structure−function relationships of the theaflavins and provide a better understanding of the role of theaflavins in biological processes. The significance of the results are discussed in the context of black tea composition and bioactivity.

KEYWORDS: Theaflavin, lipid bilayer, modeling, membrane affinity, teas

INTRODUCTION

Tea leaves produce organic compounds that may be involved in the defense of plants against invading pathogens including insects, bacteria, fungi, and viruses.[1,2] These metabolites include polyphenolic compounds, the so-called catechins in green teas. Postharvest inactivation of phenol oxidases in green tea leaves prevents oxidation of the catechins, whereas postharvest enzyme-catalyzed oxidation (fermentation) of catechins in tea leaves results in the formation of four theaflavins as well as polymeric thearubigins.[3] These substances impart the black color to black teas. Black and partly fermented oolong teas contain both classes of phenolic compounds. Teas from different sources differ widely in their content of flavonoids (polyphenolic catechins plus theaflavins).

Interest in theaflavins arises from the fact that they are reported to exhibit numerous health-related beneficial effects.[4,5] These include antiallergic,[6] antibacterial,[7−9] anticancer,[10−12] anticholesterol,[13] antidiabetic,[14] antifungal,[15] anti-inflammatory,[5,16] antitoxin,[7] antiulcer,[17] antiviral,[18] lipid-lowering,[19] and neuroprotective [20] effects.

One mechanism by which both green tea catechins and black tea theaflavins operate at the cellular−molecular level involves interaction with components of cell membranes. This leads to the prevention of binding of bioactive molecules such as enzymes to receptor sites and/or disruption of cell membranes resulting in the leakage of cell components followed by cell death.

In previous studies, we found that tea catechins have a strong affinity for the lipid bilayer of cell membranes via hydrogen bonding to the bilayer surface, with some catechins able to penetrate underneath the surface.[21,22] We suggested that large differences in the biological activities of structurally different catechins may to be due to differences in relative affinities to lipid and glycoprotein layers of cell membranes. The results indicated that hydrogen bonding of phenolic hydroxyl groups of catechins to lipid bilayers of cell membranes may govern the mechanism of antimicrobial, anticancer, and other beneficial effects of catechins.

The objective of this study was to characterize the behavior of three of the four known theaflavins depicted in Figure 1, theaflavin (TF), theaflavin-3-gallate (TF3G), and theaflavin-3,3′-digallate (TF3,3′G), as they make contact with a mixed POPC/POPE bilayer. The results are interpreted in terms of the influence of the theaflavins' structure on affinity for the bilayer, the theaflavin configurations on the bilayer surface, hydrogen bonding characteristics, molecular transport, and relationships of structure to bioactivity and to theaflavin content of black teas. To our knowledge, this is the first report on molecular modeling of affinities of theaflavins to cell membranes.

MATERIALS AND METHODS

Molecular dynamics simulations were performed for TF, TF3G, and TF3,3′G interacting with a mixed POPC/POPE lipid bilayer. All-atom molecular structures were created for the theaflavins, lipid headgroups, and water using PRODRG[23] and GROMACS software. The lipid hydrocarbon tails were treated with a united-atom CH model. Intramolecular interactions and nonbonded interactions for the lipids (Lennard-Jones and Coulombic potentials) were obtained from a previous study.[24] Short-range van der Waals and electrostatic interactions were cut off at 1.0 nm, and the particle mesh Ewald (PME) method was used to correct

Received: February 16, 2011
Accepted: March 18, 2011
Revised: March 17, 2011
Published: March 18, 2011

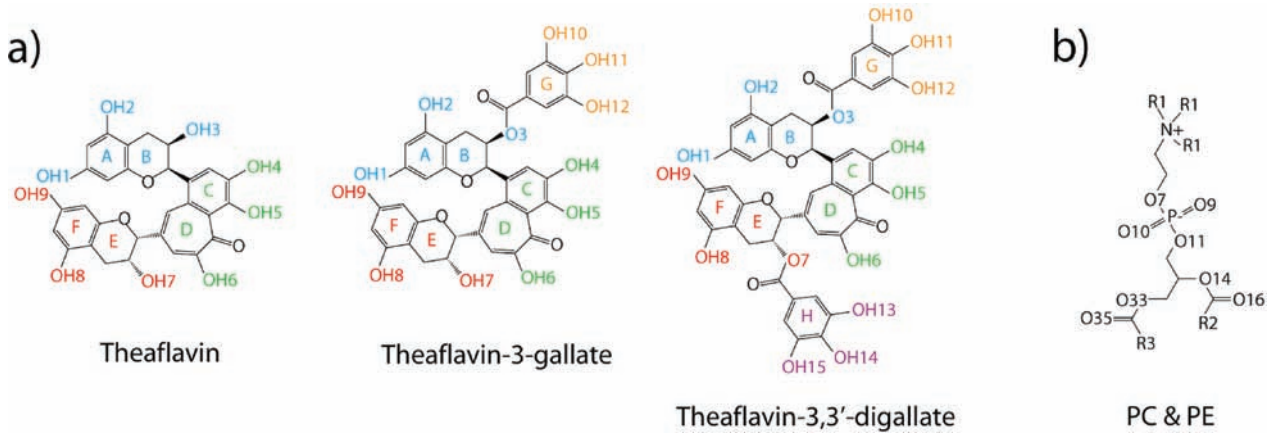

Figure 1. (a) Identification of the ring structures and functional groups in the theaflavins. Hydroxyl groups (OH1−OH15) and ring labels (A−H) for theaflavins are color coded. (b) Chemical structure of the lipid headgroup and corresponding oxygen atom numbering assignment. R_1 is CH_3 and H for PC and PE lipids, respectively. R_2 and R_3 are the oleic and palmitic acid tails, respectively.

for long-range electrostatic interactions.[25,26] The single point charge (SPC) model[27] was used for water and the OPLS forcefield for all theaflavin compounds.[28]

The molecular dynamics simulations were performed using the leapfrog integration scheme with a time step of 2 fs. The linear constraint solver (LINCS) algorithm[29] was applied to constrain all bonds in the lipids and catechins. The SETTLE algorithm[30] was applied for water molecules. All simulations were performed in the *NPT* ensemble using the Berendsen weak coupling technique and anisotropic pressure scaling[31] with periodic boundary conditions applied in all directions. The GROMACS 4.0.1 software package in single precision[32−34] was used for all simulations running in parallel on Virginia Tech's System X.

As in our earlier study, we consider model cell membranes representative of a HepG2 liver cell. The HepG2 cell membrane is approximately 75% phosphatidylcholine (PC) and phosphatidylethanolamine (PE) lipid headgroups, with six other lipids making up the other 25%.[35] The largest concentrations of fatty acids are saturated C16 (50%) and monounsaturated C18 (35%).[36] As an approximation, we considered lipid bilayers composed of a 1:1 mixture of 1-palmitoyl-2-oleoyl-phosphatidylcholine (POPC) and 1-palmitoyl-2-oleoyl- phosphatidylethanolamine (POPE).

The lipid bilayers were built by placing the lipids on a grid to form a monolayer, then transposing another monolayer to form a bilayer structure. The POPC/POPE bilayers contained 144 lipids per leaflet. A total of 11,520 water molecules (40 water/lipid) were packed around the lipid bilayer to create a fully hydrated bilayer system. The system was initially heated to 450 K for 10 ns, then cooled and equilibrated at 310 K for 50 ns.

All simulations were performed at 310 K and 100 kPa, corresponding to a liquid-crystalline state for the POPC/POPE bilayer.[24] The stability of the equilibrated bilayer was confirmed from the area per lipid (0.57 nm^2) and lipid tail order parameters. These were in agreement with previously reported values for 1:1 mixed POPC/POPE bilayers.[37] Properties of pure and mixed POPC/POPE lipid bilayers can be found elsewhere.[24,37]

The equilibrated bilayer was exposed to a solution containing a single TF, TF3G, or TF3,3′G molecule (see Figure 1 for labeling of the atoms and rings). Each of the theaflavin molecules were initially positioned in the center of the aqueous phase. Unconstrained molecular dynamics simulations were then performed for 50 ns on the systems of theaflavins, lipids, and water. To obtain a larger sample of theaflavin dynamics, five instances of each theaflavin−bilayer system were studied, for a total of 15 simulations of 50 ns each. Each theaflavin was inserted onto a plane corresponding to the center of the water phase. The initial conditions (the position on the plane and thermal velocities) were unique for each run.

RESULTS AND DISCUSSION

The lipid bilayer is likely to be the first point of contact for tea polyphenols as they interact with the cell, yet little detailed information is known about their dynamics near bilayer surfaces. Previously, we examined the binding characteristics of tea catechins with lipid membranes using molecular dynamics simulation.[21,22] Structural differences among the catechins were seen to greatly affect the nature of their interaction with the membrane surface and potentially influence the catechins' bioactivity. Theaflavin interactions with the cell membrane have not been characterized; thus, we were motivated to carry out the molecular dynamics simulations reported here. Structural differences among theaflavins, particularly the presence of one or more gallate moieties, could impact the affinity of theaflavins for the lipid bilayer due to effects of molecular size and additional hydrogen bonds formed on the gallate moieties. Understanding the influence of these structural differences is important since the biological activities of theaflavins may be related to the affinity for the bilayer or transport across the bilayer surface.

The molecular configuration and dynamics of the theaflavins were examined in each simulation. Figure 2 shows examples of the center-of-mass (COM) molecular trajectories for TF, TF3G, and TF3,3′G molecules. The trajectories show theaflavins binding to lipid headgroups near the bilayer surface. As shown in Figure 2, the theaflavins are initially inserted in the middle of the aqueous phase and quickly diffuse to interact with the bilayer. For the purposes of this study, a theaflavin−bilayer interaction is defined as the presence of at least one hydrogen bond between a theaflavin hydroxyl donor and a lipid oxygen acceptor. Trajectories of the remaining theaflavins (not shown) also have predominantly interfacial interactions with the lipid headgroups over 50 ns of simulation.

As shown by the COM trajectories in Figure 2, the theaflavins had many opportunities to bind with the bilayer throughout the simulation and interactions often started at about 5 ns. Sustained interactions with the bilayer surface lasting more than 25 ns were observed in the complete set of COM trajectories (not shown

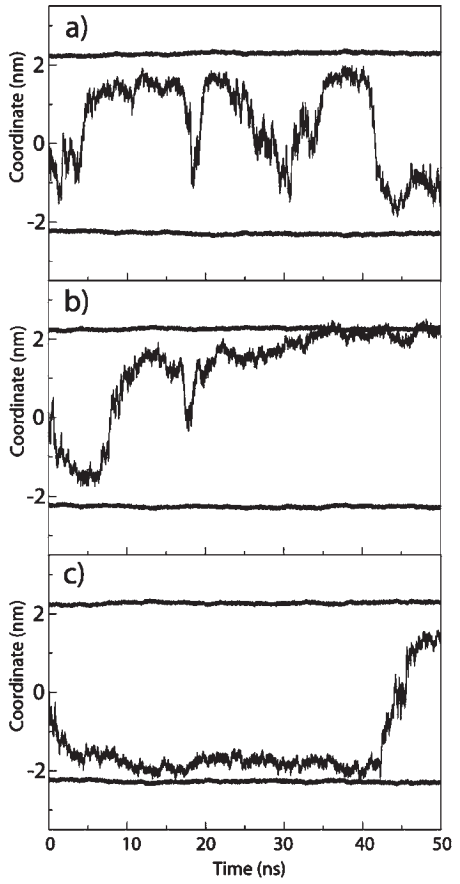

Figure 2. Sample COM trajectories for (a) TF, (b) TF3G, and (c) TF3,3′G. The solid parallel lines represent the average position of the phosphorus atoms in the lipid headgroups, position zero corresponds to the middle of the aqueous phase, and regions above and below the solid lines correspond to the lipid bilayer. Because of periodic boundary conditions, the theaflavins can interact with either bilayer surface. Note: parts of the theaflavins can be relatively far from the COM depending on the molecular orientation.

Table 1. Total Time (ns) Each Theaflavin Bound with the Bilayer Surface over the Simulation[a]

molecule	A	B	C	D	E
TF	32.7	32.5	44.7	13.9	16.0
TF3G	33.7	35.1	20.8	34.7	19.4
TF3,3′G	31.2	47.5	40.8	43.3	30.4

[a] The total time is found by summing each time interval that an H-bond is formed with the bilayer. Symbols A−E represent the five simulations for each theaflavin.

here) for three of the TF trajectories, two of the TF3G trajectories, and all five of the TF3,3′G trajectories. The total time that individual theaflavins interacted with the bilayer surface is shown in Table 1. TF and TF3G molecules had similar interaction times (average of 28.0 and 28.7 ns, respectively), but TF3,3′G molecules interacted for longer times (average of 38.6 ns).

The ability of the theaflavins to remain bound to the bilayer is likely linked to their configuration on the bilayer surface and may be an important factor for their bioactivity. The theaflavins' position and orientation on the bilayer was inferred from the trajectories

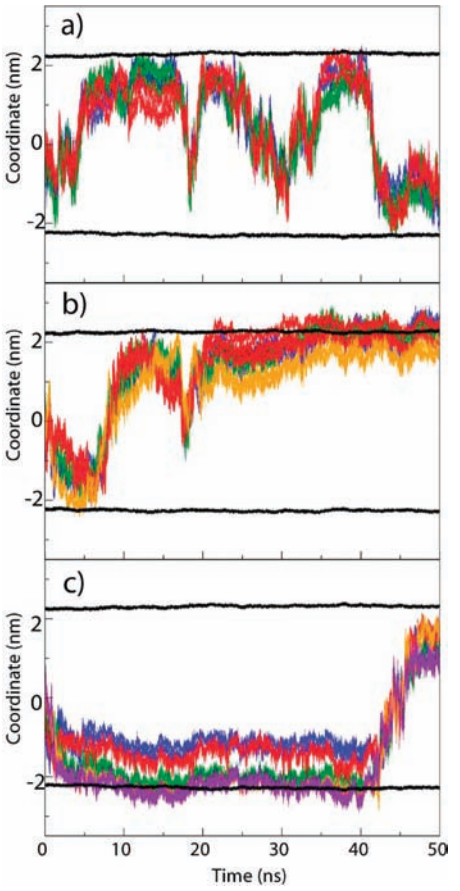

Figure 3. Trajectory of the hydroxyl oxygen for a simulation of (a) TF, (b) TF3G, and (c) TF3,3′G. Each hydroxyl oxygen is color-coded to correspond to a molecular plane on the theaflavin. The key is shown in Figure 1.

of theaflavin hydroxyl oxygen atoms. A sample set of trajectories for the hydroxyl oxygen of TF, TF3G, and TF3,3′G is shown in Figure 3; these correspond to the COM trajectories shown in Figure 2. The hydroxyl oxygens are color-coded to correspond to a molecular plane on the theaflavin molecules (see Figure 1 for the key).

The trajectories of the hydroxyl oxygens indicate that the theaflavins can vary their orientation on the bilayer surface or remain in a relatively unchanging configuration. Patterns emerged regarding the positions of the molecular rings. TF often interacted with the bilayer on two molecular planes, with the C/D ring often one of the two in contact. In the five TF simulations, the amount of time TF spent on the bilayer varied from about 14 to 45 ns (of 50 ns possible). Figure 3a shows the trajectory of a TF molecule that interacted with the bilayer repeatedly, but did not remain bound to the surface for more than 5 ns before releasing into the aqueous phase. This contrasts with the two sample trajectories of TF3G and TF3,3′G shown in Figure 3b and c, respectively. In these trajectories, both molecules were bound for most of the simulation and maintained a near-constant configuration during long interactions. In the five TF3G simulations, the gallate moiety of TF3G remained in the aqueous phase during the two longest bilayer interactions (Figure 3b shows the longest TF3G interaction). TF3,3′G demonstrated a tendency for the C/D ring to be farthest from the bilayer surface during four of the five trajectories (e.g., Figure 3c). TF3,3′G molecules remained in

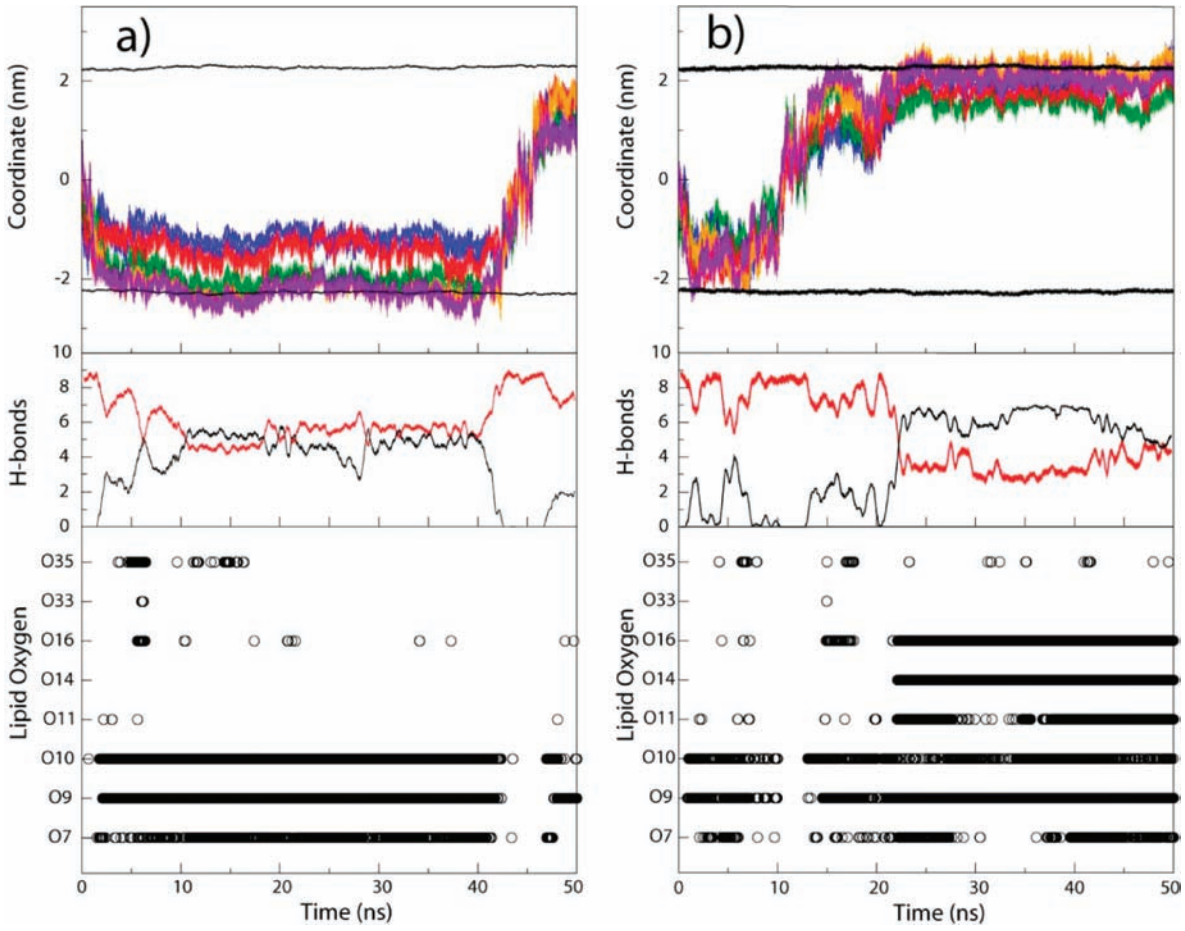

Figure 4. Comparison of the molecular binding of TF3,3′G when (a) three planes are in contact with the bilayer and (b) four planes are in contact. Upper panel: trajectory of each hydroxyl oxygen of the theaflavin. Middle panel: the average number of H-bonds formed simultaneously with water (black) and lipid oxygen (red). Lower panel: H-bonds formed between hydroxyl donors groups of TF3,3′G and oxygen acceptors of the lipids. Each circle represents an H-bond formed between TF3,3′G and a specific lipid oxygen acceptor. See Figure 1 for the labeling of lipid oxygen atoms.

a near-constant configuration on the bilayer surface consecutively for 25 ns or more in four of the five TF3,3′G trajectories (e.g., Figure 3c).

A detailed analysis of the hydrogen bonding between the theaflavins and lipids was performed to help understand their interactions along the bilayer interface. A hydrogen bond is defined as the distance between the H-donor and H-acceptor of <0.35 nm and a donor−hydrogen−acceptor angle between 120 and 180°.[38] This analysis considered theaflavin hydroxyl groups as H-bond donors and lipid oxygen groups as H-bond acceptors. The naming assignments for atoms in the lipid headgroups and theaflavins are found in Figure 1.

The number and characteristics of the theaflavin−lipid H-bonds were examined closely for each simulation. As an example, Figure 4 shows the hydroxyl trajectories of two TF3,3′G molecules (top chart) and their corresponding H-bond behavior (middle and lower chart). The middle chart of Figure 4 shows the number of H-bonds formed simultaneously by TF3,3′G with the bilayer (black) and with water (red) during the trajectory. The lower chart shows the lipid oxygen acceptors that are engaged in H-bonds with the theaflavins. The common binding configurations of TF3,3′G are shown in Figure 4. In Figure 4a, the C/D ring is near the bilayer surface, and in Figure 4b, the C/D ring is near the aqueous phase.

For every theaflavin molecule, a majority of the hydroxyl donors were engaged in H-bonds with either the bilayer or water throughout the trajectories. As demonstrated in Figure 4a and b, H-bonds are first formed only with water (while the theaflavins are solely in the aqueous phase). As the theaflavin approaches the bilayer, H-bonds are formed with lipid oxygen.

The H-bond acceptors in bilayer and water seemed to compete for the H-bond donors in the theaflavins. For example, at approximately 22 ns in Figure 4b, the TF3,3′G molecule begins to bind to the bilayer. The H-bonds simultaneously formed with the bilayer increased to about six, while the H-bonds with the water reduce to about three. A similar competition for hydroxyl H-bond donors was observed in all of the simulations, presumably because a move from the aqueous phase to the bilayer surface breaks H-bonds formed with water molecules and forms a similar number of H-bonds with lipid oxygen.

Table 2 provides a summary of the number of H-bonds formed simultaneously with water and lipid oxygen as the theaflavins interacted with the bilayer. On average, all three theaflavins formed more simultaneous H-bonds with water oxygen than with lipid oxygen while bound to the bilayer surface. For example, 4.9 hydroxyl groups in TF (about 55%) were involved in H-bonds with water oxygen, while only 1.4 (about 16%) hydroxyl groups formed H-bonds with lipid oxygen. The remaining hydroxyl groups were either not engaged in H-bonds or formed intramolecular H-bonds.

Table 2. Number of Simultaneous H-Bonds Occurring between the Theaflavin Hydroxyl Groups and the Water or Lipid Oxygen while the Theaflavins Were on the Bilayer Surface[a]

molecule	H-bonds	A	B	C	D	E	AVE	OH	AVE/OH
TF	water	5.040	5.122	4.567	N/A	N/A	4.910	9	0.546
TF	LO	1.153	1.175	1.899	N/A	N/A	1.409	9	0.157
TF3G	water	5.962	5.243	N/A	5.207	N/A	5.471	11	0.497
TF3G	LO	1.395	0.955	N/A	1.528	N/A	1.293	11	0.118
TF3,3′G	water	7.359	4.245	5.371	6.142	6.659	5.955	13	0.458
TF3,3′G	LO	1.863	5.525	3.937	3.654	1.303	3.256	13	0.250

[a] AVE indicates average values; OH is the number of hydroxyl groups for each theaflavin; AVE/OH is the fraction of hydroxyl groups involved in H-bonds with the lipid oxygen (LO) or water. To ensure a large sample size, only sustained interactions of 25 ns or more are considered (others are marked with N/A).

The number of hydroxyl groups forming H-bonds with water increased as the total number of hydroxyl groups in the theaflavins increased (TF < TF3G < TF3,3′G). However, the number of H-bonds formed with the bilayer was similar for TF and TF3G (about 1.4 and 1.3, respectively) but much greater for TF3,3G (about 3.3). TF3,3′G not only did form the greatest absolute number of H-bonds with the bilayer but also utilized the largest fraction of its hydroxyl donor groups (25%) compared with TF and TF3G (16% and 12%, respectively).

The behavior of TF3,3′G was examined more closely to better understand its greater ability to bind with the bilayer. The two TF3,3′G trajectories that formed the greatest number of H-bonds with the bilayer occurred where four molecular planes of TF3,3′G (rings A/B, E/F, G, and H) were near the bilayer surface. Other configurations were effective at binding TF3,3′G to the bilayer surface but produced fewer H-bonds with lipid oxygen, thus suggesting a weaker interaction. The TF3,3′G trajectories shown in Figure 4 depict two observed configurations of TF3,3′G. Figure 4a shows three molecular planes (rings C/D, G, and H) on the bilayer surface, and Figure 4b shows four molecular planes (rings A/B, E/F, G, and H) on the bilayer surface. Both configurations resulted in the TF3,3′G molecule remaining on the bilayer. The configuration of Figure 4a produced H-bonds with phosphate oxygen acceptors (O7, O9, O10, and O11) near the bilayer surface, while the configuration in Figure 4b produced H-bonds with acceptors both on the surface and deeper inside the bilayer (O14 and O16). The precise depth that theaflavin rings penetrate the bilayer cannot be determined from trajectories like that of Figure 4 since the position of the bilayer represents the average position of the bilayer surface. However, observations corresponding to Figure 4b show that the two gallate moieties (rings G, H) penetrated below the lipid phosphate oxygen into positions that allow H-bonds with acceptors O11, O14, and O16.

Mechanistic Aspects. The structures of the test substances differ as follows: TF has no gallate side chain, TF3G has one, and TF3,3′G has two. The presence of one gallate moiety (in TF3G) does not seem to impact the binding time with the bilayer relative to TF. By contrast, the presence of two gallate moieties (in TF3,3′G) increased the average binding time by about 11 ns over 50 ns simulations. Also, TF and TF3G intermittently bound and released from the bilayer, while TF3,3′G was more likely to remain bound. The ability of TF3,3′G to stay on the bilayer for a substantially longer time than TF or TF3G is likely linked to its ability to utilize a larger percent of its hydroxyl groups for H-bonds with the bilayer.

TF3,3′G exhibited several configurations while bound to the bilayer. One common configuration had four molecular planes (rings A/B, E/F, G, H) directed toward the bilayer surface; this configuration generated the greatest number of simultaneous H-bonds. The high degree of hydrogen bonding for TF3,3′G in all of the simulations can be explained by the large number of hydroxyl groups that are accessible to the bilayer, even in configurations shown Figure 4a that are less optimal for bilayer H-bonds. TF3,3′G hydroxyl groups are accessible both as a result of the orientation of the theaflavin planes and their penetration into the bilayer, especially rings G and H.

During bilayer interactions, the gallate moiety of TF3G was often positioned in the aqueous phase, rather than the lipid phase. Since the gallate moiety has a high density of hydroxyl groups (three) and is more polar than the other parts of the TF3G molecule, this positioning likely limited the number of H-bonds that occurred simultaneously with the bilayer. The percentage of TF3G hydroxyl groups forming H-bonds with the bilayer was the smallest of the three theaflavins, further suggesting that the molecular structure is not ideal for H-bonding under the conditions studied here. This study did not explore the other theaflavin monogallate, TF3′G.

These results suggest that the chemical functionality provided by rings G and H (the two gallate moieties) greatly influence interactions with the lipid bilayer. The presence of two gallate moieties in TF3,3′G allows a configuration on the bilayer that efficiently forms H-bonds; a similar configuration is not possible in TF and TF3G.

The degree of affinity for the lipid bilayer could affect the transport, distribution, and bioactivity of theaflavins in vivo. TF3,3′G showed a stronger ability to inhibit the growth of fibroblasts and carcinoma cells than did TF and TF3G, which had similar abilities.[39] The authors indicate that the inhibition of tumor growth by black tea might occur through the suppression of extracellular signals and that TF3,3′G was the strongest inhibitor in black tea. Signal inhibition processes involve cellular interactions where the theaflavins' affinity for the lipid bilayer is potentially important since theaflavins that bind with the bilayer have an opportunity to be delivered to membrane proteins that are potentially linked with apoptosis, rather than drifting away from the cell in the aqueous phase. One characteristic that may influence the effectiveness of TF3,3′G, compared with TF and TF3G, is the ability to remain bound with lipid bilayers without being absorbed into the interior of the bilayer.

A related study[18] showed that computer-aided molecular docking of TF3,3′G may bind to the highly conserved hydrophobic pocket on the surface of the HIV-1 virus. Theaflavins had more potent anti-HIV-1 activity than catechins. The authors suggest that theaflavin derivatives may serve as HIV-1 entry inhibitors.

It should be noted that the time scale studied here (50 ns) is only appropriate for studying the initial interaction with the bilayer but is not long enough to address absorption into the bilayer, diffusion, or other phenomena requiring longer simulations. Because we have previously observed the reduced absorption of green tea catechins with increasing molecular size,[22] the larger size of TF3,3′G relative to TF and TF3G may reduce or inhibit absorption. Counteracting the size effect, the larger functionality and polarity provided by the two gallate moieties result in the observed strong interaction with lipid headgroups.

TF3,3′G is thought to be pharmacologically the most potent of the theaflavins and is sometimes used to represent the bioactivity

of all the theaflavins in black tea.[8,40] The results presented here provide detailed observations of theaflavin−membrane interactions and help to explain the experimentally observed antibacterial and anticarcinogenic potency of TF3,3′G and distinguish its behavior from the other theaflavins.

Theaflavin Content of Black Teas. Black tea represents a rich source of antioxidative phenolic compounds.[41] The literature suggests that geographical origin, soil composition, differences in the composition of different leaves, time of harvesting, postharvest treatments, and physical structure of the different leaves probably influence the composition of tea leaves. Also contributing to this variability is the susceptibility of tea compounds to extraction by different solvents[42−44] as well as long-term storage.[45] For example, we reported that significantly greater quantities of individual and total flavonoids (catechins and theaflavins) were extracted with 80% ethanol/water at 60 °C for 15 min than with boiled water for 5 min from 77 commercial teas sold in the United States.[46,47] The latter conditions are widely used in the home to prepare tea infusions. The distribution of the individual catechins and theaflavins in individual teas extracted by the two solvents also varied. The following ranges of concentrations of flavonoids (catechins plus theaflavins) in the tea leaves extracted with 80% ethanol were observed (in mg/g): in 32 black teas, 19.8−115.1; in 24 green teas, 12.3−136.3; and in 14 specialty teas, 4.9−118.5.

A related study[48] reported that the content of individual and total theaflavins in four teas ranged as follows: TF, from 1.24 to 2.26; TF3G, from 0.97 to 3.59; TF3′G, from 0.63 to 2.27; TF3,3′G, from1.54 to 11.31; sum, from 4.28 to 19.07. These observations suggest that consumers have a choice of selecting individual black teas with high content of biologically more active TF3,3′G as well as total theaflavin content.

Bioavailability and Bioactivity Aspects. Although the bioavailability (absorption from the digestive tract into the circulation and distribution to various organs) of tea flavonoids is low, multiple consumption of teas resulted in significant accumulation of catechins in most body organs with relatively high peak plasma levels.[49−52] Because micromolar levels of tea compounds can exhibit bioactivity in vitro and in vivo, the human bioavailability data suggest that long-term consumptions of tea can result in the absorption and retention of sufficient amounts of flavonoids to exert antimicrobial and other beneficial effects directly in plasma and tissues or indirectly by modulating cell signaling pathways. The bioavailability of individual theaflavins has thus far apparently not been evaluated in human studies.

.In conclusion, the results of the present study indicate that the mechanism of action of black tea theaflavins at the molecular and cell membrane levels appears to be similar to that we previously found for green tea catechins. The findings are consistent with reported relative bioactivities (potencies) of structurally different theaflavins. Finally, it would be of interest to apply the described molecular modeling approach to other polyphenolic compounds present in teas,[53] to mixtures of catechins and theaflavins of commercial and newly developed teas,[54] and to other plant foods, including onions[55] and sweet potatoes,[56] in order to determine whether the results can predict bioactivities.[57]

AUTHOR INFORMATION

Corresponding Author

*Tel: 410-306-1305. Fax: 410-306-0676 E-mail: tim.sirk@us.army.mil.

ACKNOWLEDGMENT

Computational resources were provided by the Virginia Tech Advanced Research Computing Facility (System X). We thank Carol E. Levin for assistance with the manuscript as well as Amadeu Sum (Colorado School of Mines) for his helpful discussions on modeling and analysis.

ABBREVIATIONS USED

COM, center-of-mass; LINCS, linear constraint solver; NPT, number particle temperature; OPC, 1-palmytoyl-2-oleoyl-phosphatidylcholine; OPLS, optimized potential for liquid simulation; PC, phosphatidylcholine; PE, phosphatidylethanolamine; POPE, 1-palmytoyl-2-oleoyl- phosphatidylethanolamine; PME, particle mesh Ewald; SPC, single point charge; TF, theaflavin; TF3G, theaflavin-3-gallate; TF3′, theaflavin-3′-gallate; TF3,3′G, theaflavin-3.3′-digallate.

REFERENCES

(1) Ho, C.-T.; Lin, J.-K.; Shahidi, F. *Tea and Tea Products: Chemistry and Health-Promoting Properties*; CRC Press: Boca Raton, FL, 2009; p 305.

(2) Chiu, S. Is green tea really good for you?. *J. Food Sci. Educ.* **2006**, *5*, 70–71.

(3) Tanaka, T.; Miyata, Y.; Tamaya, K.; Kusano, R.; Matsuo, Y.; Tamaru, S.; Tanaka, K.; Matsui, T.; Maeda, M.; Kouno, I. Increase of theaflavin gallates and thearubigins by acceleration of catechin oxidation in a new fermented tea product obtained by the tea-rolling processing of loquat (*Eriobotrya japonica*) and green tea leaves. *J. Agric. Food Chem.* **2009**, *57*, 5816–5822.

(4) Gupta, J.; Siddique, Y. H.; Beg, T.; Ara, G.; Afzal, M. A review on the beneficial effects of tea polyphenols on human health. *Int. J. Pharmacol.* **2008**, *4*, 314–338.

(5) de Mejia, E. G.; Ramirez-Mares, M. V.; Puangpraphant, S. Bioactive components of tea: Cancer, inflammation and behavior. *Brain Behav. Immun.* **2009**, *23*, 721–731.

(6) Yoshino, K.; Yamazaki, K.; Sano, M. Preventive effects of black tea theaflavins against mouse type IV allergy. *J. Sci. Food Agric.* **2010**, *90*, 1983–1987.

(7) Friedman, M. Overview of antibacterial, antitoxin, antiviral, and antifungal activities of tea flavonoids and teas. *Mol. Nutr. Food Res.* **2007**, *51*, 116–134.

(8) Friedman, M.; Henika, P. R.; Levin, C. E.; Mandrell, R. E.; Kozukue, N. Antimicrobial activities of tea catechins and theaflavins and tea extracts against *Bacillus cereus*. *J. Food Prot.* **2006**, *69*, 354–361.

(9) Juneja, V. K.; Bari, M. L.; Inatsu, Y.; Kawamoto, S.; Friedman, M. Thermal destruction of *Escherichia coli* O157:H7 in sous-vide cooked ground beef as affected by tea leaf and apple skin powders. *J. Food Prot.* **2009**, *72*, 860–865.

(10) Kaur, S.; Greaves, P.; Cooke, D. N.; Edwards, R.; Steward, W. P.; Gescher, A. J.; Marczylo, T. H. Breast cancer prevention by green tea catechins and black tea theaflavins in the C3(1) SV40 T,t antigen transgenic mouse model is accompanied by increased apoptosis and a decrease in oxidative DNA adducts. *J. Agric. Food Chem.* **2007**, *55*, 3378–3385.

(11) Adhikary, A.; Mohanty, S.; Lahiry, L.; Hossain, D. M. S.; Chakraborty, S.; Das, T. Theaflavins retard human breast cancer cell migration by inhibiting NF-κB via p53-ROS cross-talk. *FEBS Lett.* **2010**, *584*, 7–14.

(12) Friedman, M.; Mackey, B. E.; Kim, H. J.; Lee, I. S.; Lee, K. R.; Lee, S. U.; Kozukue, E.; Kozukue, N. Structure-activity relationships of tea compounds against human cancer cells. *J. Agric. Food Chem.* **2007**, *55*, 243–253.

(13) Vermeer, M. A.; Mulder, T. P.; Molhuizen, H. O. Theaflavins from black tea, especially theaflavin-3-gallate, reduce the incorporation of cholesterol into mixed micelles. *J. Agric. Food Chem.* **2008**, *56*, 12031–12036.

(14) Hayashino, Y.; Fukuhara, S.; Okamura, T.; Tanaka, T.; Ueshima, H. High oolong tea consumption predicts future risk of diabetes among Japanese male workers: a prospective cohort study. *Diabet. Med.* **2011**10.1111/j.1464-5491.2011.03239.x.

(15) Sitheeque, M. A. M.; Panagoda, G. J.; Yau, J.; Amarakoon, A. M. T.; Udagama, U. R. N.; Samaranayake, L. P. Antifungal activity of black tea polyphenols (catechins and theaflavins) against *Candida* species. *Chemotherapy* **2009**, *55*, 189–196.

(16) Hosokawa, Y.; Hosokawa, I.; Ozaki, K.; Nakanishi, T.; Nakae, H.; Matsuo, T. Tea polyphenols inhibit IL-6 production in tumor necrosis factor superfamily 14-stimulated human gingival fibroblasts. *Mol. Nutr. Food Res.* **2010**, *54* (Suppl 2), S151–S158.

(17) Adhikary, B.; Yadav, S. K.; Roy, K.; Bandyopadhyay, S. K.; Chattopadhyay, S. Black tea and theaflavins assist healing of indomethacin-induced gastric ulceration in mice by antioxidative action. *Evid. Based Complement. Alternat. Med.* **2011**, *2011*, 1–11.

(18) Liu, S.; Lu, H.; Zhao, Q.; He, Y.; Niu, J.; Debnath, A. K.; Wu, S.; Jiang, S. Theaflavin derivatives in black tea and catechin derivatives in green tea inhibit HIV-1 entry by targeting gp41. *Biochim. Biophys. Acta* **2005**, *1723*, 270–281.

(19) Lin, C.-L.; Huang, H.-C.; Lin, J.-K. Theaflavins attenuate hepatic lipid accumulation through activating AMPK in human HepG2 cells. *J. Lipid Res.* **2007**, *48*, 2334–2343.

(20) Bastianetto, S.; Yao, Z.-X.; Papadopoulos, V.; Quirion, R. Neuroprotective effects of green and black teas and their catechin gallate esters against β-amyloid-induced toxicity. *Eur. J. Neurosci.* **2006**, *23*, 55–64.

(21) Sirk, T. W.; Brown, E. F.; Sum, A. K.; Friedman, M. Molecular dynamics study on the biophysical interactions of seven green tea catechins with lipid bilayers of cell membranes. *J. Agric. Food Chem.* **2008**, *56*, 7750–7758.

(22) Sirk, T. W.; Brown, E. F.; Friedman, M.; Sum, A. K. Molecular binding of catechins to biomembranes: relationship to biological activity. *J. Agric. Food Chem.* **2009**, *57*, 6720–6728.

(23) Schüttelkopf, A. W.; Van Aalten, D. M. F. PRODRG: A tool for high-throughput crystallography of protein-ligand complexes. *Acta Crystallogr., Sect. D* **2004**, *60*, 1355–1363.

(24) Leekumjorn, S.; Wu, Y.; Sum, A. K.; Chan, C. Experimental and computational studies investigating trehalose protection of HepG2 cells from palmitate-induced toxicity. *Biophys. J.* **2008**, *94*, 2869–2883.

(25) Darden, T.; York, D.; Pedersen, L. Particle mesh Ewald: An N·log(N) method for Ewald sums in large systems. *J. Chem. Phys.* **1993**, *98*, 10089–10092.

(26) Essmann, U.; Perera, L.; Berkowitz, M. L.; Darden, T.; Lee, H.; Pedersen, L. G. A smooth particle mesh Ewald method. *J. Chem. Phys.* **1995**, *103*, 8577–8593.

(27) Berendsen, H. J. C.; Postma, J. P. M.; Van Gunsteren, W. F.; Hermans, J. Interaction Models for Water in Relation to Protein Hydration. In *Intermolecular Forces*; Pullman, B., Ed.; D. Reidel Publishing Co.: Dordrecht, The Netherlands, 1981; pp 331−342.

(28) Jorgensen, W. L.; Maxwell, D. S.; Tirado-Rives, J. Development and testing of the OPLS all-atom force field on conformational energetics and properties of organic liquids. *J. Am. Chem. Soc.* **1996**, *118*, 11225–11236.

(29) Mazur, A. K. Quasi-Hamiltonian equations of motion for internal coordinate molecular dynamics of polymers. *J. Comput. Chem.* **1997**, *18*, 1354–1364.

(30) Miyamoto, S.; Kollman, P. A. SETTLE: An analytical version of the SHAKE and RATTLE algorithms for rigid water models. *J. Comput. Chem.* **1992**, *13*, 952–962.

(31) Berendsen, H. J. C.; Postma, J. P. M.; Van Gunsteren, W. F.; Dinola, A.; Haak, J. R. Molecular dynamics with coupling to an external bath. *J. Chem. Phys.* **1984**, *81*, 3684–3690.

(32) Lindahl, E.; Hess, B.; van der Spoel, D. GROMACS 3.0: A package for molecular simulation and trajectory analysis. *J. Mol. Model.* **2001**, *7*, 306–317.

(33) Berendsen, H. J. C.; van der Spoel, D.; van Drunen, R. GROMACS: a message-passing parallel molecular dynamics implementation. *Comput. Phys. Commun.* **1995**, *91*, 43–56.

(34) Van Der Spoel, D.; Lindahl, E.; Hess, B.; Groenhof, G.; Mark, A. E.; Berendsen, H. J. C. GROMACS: Fast, flexible, and free. *J. Comput. Chem.* **2005**, *26*, 1701–1718.

(35) Koumanov, K. S.; Momchilova-Pankova, A. B.; Wang, S. R.; Infante, R. Membrane phospholipid composition, fluidity and phospholipase A2 activity of human hepatoma cell line HepG2. *Int. J. Biochem.* **1990**, *22*, 1453–1455.

(36) de la Maza, M. P.; Hirsch, S.; Nieto, S.; Petermann, M.; Bunout, D. Fatty acid composition of liver total lipids in alcoholic patients with and without liver damage. *Alcohol.: Clin. Exp. Res.* **1996**, *20*, 1418–1422.

(37) Leekumjorn, S.; Sum, A. K. Molecular characterization of gel and liquid-crystalline structures of fully hydrated POPC and POPE bilayers. *J. Phys. Chem. B* **2007**, *111*, 6026–6033.

(38) Brady, J. W.; Schmidt, R. K. The role of hydrogen bonding in carbohydrates: Molecular dynamics simulations of maltose in aqueous solution. *J. Phys. Chem.* **1993**, *97*, 958–966.

(39) Liang, Y.-C.; Chen, Y.-C.; Lin, Y.-L.; Lin-Shiau, S.-Y.; Ho, C.-T.; Lin, J.-K. Suppression of extracellular signals and cell proliferation by the black tea polyphenol, theaflavin-3,3′-digallate. *Carcinogenesis* **1999**, *20*, 733–736.

(40) Schuck, A. G.; Ausubel, M. B.; Zuckerbraun, H. L.; Babich, H. Theaflavin-3,3′-digallate, a component of black tea: an inducer of oxidative stress and apoptosis. *Toxicol. in Vitro* **2008**, *22*, 598–609.

(41) Rechner, A. R.; Wagner, E.; Van Buren, L.; Van de Put, F.; Wiseman, S.; Rice-Evans, C. A. Black tea represents a major source of dietary phenolics among regular tea drinkers. *Free Radical Res.* **2002**, *36*, 1127–1135.

(42) Lin, Y. S.; Tsai, Y. J.; Tsay, J. S.; Lin, J. K. Factors affecting the levels of tea polyphenols and caffeine in tea leaves. *J. Agric. Food Chem.* **2003**, *51*, 1864–1873.

(43) Astill, C.; Birch, M. R.; Dacombe, C.; Humphrey, P. G.; Martin, P. T. Factors affecting the caffeine and polyphenol contents of black and green tea infusions. *J. Agric. Food Chem.* **2001**, *49*, 5340–5347.

(44) Wang, H.; Helliwell, K.; You, X. Isocratic elution system for the determination of catechins, caffeine and gallic acid in green tea using HPLC. *Food Chem.* **2000**, *68*, 115–121.

(45) Friedman, M.; Levin, C. E.; Lee, S.-U.; Kozukue, N. Stability of green tea catechins in commercial tea leaves during storage for 6 months. *J. Food Sci.* **2009**, *74*, H47–H51.

(46) Friedman, M.; Kim, S.-Y.; Lee, S.-J.; Han, G.-P.; Han, J.-S.; Lee, R.-K.; Kozukue, N. Distribution of catechins, theaflavins, caffeine, and theobromine in 77 teas consumed in the United States. *J. Food Sci.* **2005**, *70*, C550–559.

(47) Friedman, M.; Levin, C. E.; Choi, S.-H.; Kozukue, E.; Kozukue, N. HPLC analysis of catechins, theaflavins, and alkaloids in commercial teas and green tea dietary supplements: comparison of water and 80% ethanol/water extracts. *J. Food Sci.* **2006**, *71*, C328–337.

(48) Nishimura, M.; Ishiyama, K.; Watanabe, A.; Kawano, S.; Miyase, T.; Sano, M. Determination of theaflavins including methylated theaflavins in black tea leaves by solid-phase extraction and HPLC analysis. *J. Agric. Food Chem.* **2007**, *55*, 7252–7257.

(49) Swezey, R. R.; Aldridge, D. E.; LeValley, S. E.; Crowell, J. A.; Hara, Y.; Green, C. E. Absorption, tissue distribution and elimination of 4-[(3)h]-epigallocatechin gallate in beagle dogs. *Int. J. Toxicol.* **2003**, *22*, 187–193.

(50) Chow, H.-H. S.; Hakim, I. A.; Vining, D. R.; Crowell, J. A.; Ranger-Moore, J.; Chew, W. M.; Celaya, C. A.; Rodney, S. R.; Hara, Y.; Alberts, D. S. Effects of dosing condition on the oral bioavailability of green tea catechins after single-dose administration of polyphenon E in healthy individuals. *Clin. Cancer Res.* **2005**, *11*, 4627–4633.

(51) Doucas, H.; Garcea, G.; Neal, C. P.; Manson, M. M.; Berry, D. P. Chemoprevention of pancreatic cancer: a review of the molecular pathways involved, and evidence for the potential for chemoprevention. *Pancreatology* **2006**, *6*, 429–439.

(52) Henning, S. M.; Choo, J. J.; Heber, D. Nongallated compared with gallated flavan-3-ols in green and black tea are more bioavailable. *J. Nutr.* **2008**, *138*, 1529S–1534S.

(53) Lin, L. Z.; Chen, P.; Harnly, J. M. New phenolic components and chromatographic profiles of green and fermented teas. *J. Agric. Food Chem.* **2008**, *56*, 8130–8140.

(54) Friedman, M.; Levin, C. E.; Choi, S.-H.; Lee, S.-U.; Kozukue, N. Changes in the composition of raw tea leaves from the Korean Yabukida plant during high-temperature processing to pan-fried Kamairi-cha green tea. *J. Food Sci.* **2009**, *74*, C406–C412.

(55) Lee, S. U.; Lee, J. H.; Choi, S. H.; Lee, J. S.; Ohnisi-Kameyama, M.; Kozukue, N.; Levin, C. E.; Friedman, M. Flavonoid content in fresh, home-processed, and light-exposed onions and in dehydrated commercial onion products. *J. Agric. Food Chem.* **2008**, *56*, 8541–8548.

(56) Jung, J.-K.; Lee, S.-U.; Kozukue, N.; Levin, C. E.; Friedman, M. Distribution of phenolic compounds and antioxidative activities in parts of sweet potato (*Ipomoea batata* L.) plants and in home processed roots. *J. Food Compos. Anal.* **2011**, *24*, 29–37.

(57) Finotti, E.; Bersani, E.; Friedman, M. Application of a functional mathematical index for antibacterial and anticarcinogenic effects of tea catechins. *J. Agric. Food Chem.* **2011**, *59*, 864–869.